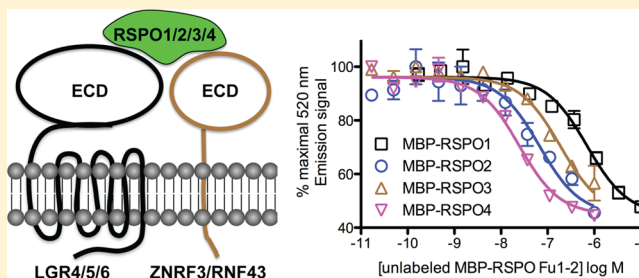# Reconstitution of R-Spondin:LGR4:ZNRF3 Adult Stem Cell Growth Factor Signaling Complexes with Recombinant Proteins Produced in *Escherichia coli*

Heather E. Moad and Augen A. Pioszak*

Department of Biochemistry and Molecular Biology, The University of Oklahoma Health Sciences Center, Oklahoma City, Oklahoma 73104, United States

**S** Supporting Information

**ABSTRACT:** R-Spondins are secreted glycoproteins (RSPO1−RSPO4) that have proliferative effects on adult stem cells by potentiating Wnt signaling. RSPO actions are mediated by the leucine-rich repeat (LRR)-containing seven-transmembrane receptors LGR4−LGR6 and the transmembrane E3 ubiquitin ligases ZNRF3 and RNF43. Here, we present a methodology for the bacterial expression and purification of the signaling competent, cysteine-rich Fu1−Fu2 domains of the four human RSPOs, a fragment of the human LGR4 extracellular domain (ECD) containing LRR1−



14, and the human ZNRF3 ECD. In a cell-based signaling assay, the nonglycosylated RSPOs enhanced low-dose Wnt3a signaling with potencies comparable to those of mammalian cell-produced RSPOs and RSPO2 and -3 were more potent than RSPO1 and -4. LGR4 LRR1−14 and ZNRF3 ECD inhibited RSPO2-enhanced Wnt3a signaling. The RSPOs bound LGR4 LRR1−14 with nanomolar affinities that decreased in the following order in a time-resolved fluorescence resonance energy transfer (TR-FRET) assay: RSPO4 > RSPO2 > RSPO3 > RSPO1. RSPO−receptor interactions were further characterized with a native gel electrophoretic mobility shift assay, which corroborated the RSPO-LGR4 TR-FRET results and indicated that RSPOs weakly bound ZNRF3 with affinities that decreased in the following order: RSPO2 > RSPO3 > RSPO1. RSPO4:ZNRF3 complexes were not detected. Lastly, ternary RSPO:LGR4:ZNRF3 complexes were detected for RSPO2 and -3. Our results indicate that RSPO and LGR4 *N*-glycans are dispensable for function, demonstrate RSPO-mediated ternary complex formation, and suggest that the stronger signaling potencies of RSPO2 and -3 result from their strong binding of both receptors. Our unique protein production methodology may provide a cost-effective source of recombinant RSPOs for regenerative medicine applications.

R-Spondins make up a vertebrate family of four secreted glycoproteins (RSPO1−RSPO4) that regulate Wnt signaling to effect development in embryonic and adult tissues.[1−4] RSPO2 was identified as an activator of Wnt/$\beta$-catenin signaling in an expression screen,[5] and RSPO1 was shown to exhibit potent mitogenic effects on intestinal epithelium *in vivo*[6] and on Wnt-dependent adult stem cell compartments *in vitro*.[7,8] RSPOs function by potentiating Wnt signaling; i.e., the potency of Wnt signals is enhanced in the presence of RSPOs. As a consequence of their function as growth factors for adult stem cells, RSPOs have received considerable attention for regenerative medicine applications. Exogenous RSPO1 is a crucial component of *in vitro* cell culture systems that allow the growth of intestinal organoids from adult stem cells.[8,9] RSPOs are also of interest for their roles in cancer. Aberrant expression of RSPO2 or -3 is implicated as a driver of tumorigenesis in colon cancers.[10] In addition, RSPO1 and -4 mutations are found in the human developmental disorders female-to-male sex reversal[11] and anonychia,[12−14] respectively.

The four RSPOs are ~40−60% identical in amino acid sequence. Their domain structure consists of an N-terminal signal peptide followed by two cysteine-rich Furin-like domains, Fu1 and Fu2, a thrombospondin domain, and a C-terminal basic region. The Fu1−Fu2 domain fragment is minimally sufficient to potentiate Wnt signaling.[5] Leucine-rich repeat (LRR)-containing seven-transmembrane (7-TM) receptors LGR4−LGR6 were the first *bona fide* RSPO receptors identified that mediate their enhancement of Wnt signals.[15−18] LGR5 marks adult stem cells of the intestine, colon, stomach, hair follicle, and liver,[19−22] and LGR6 marks adult stem cells of the epidermis.[23] LGR4 is not restricted to stem cells but is co-expressed with LGR5 in intestinal crypt stem cells.[16] LGR4−LGR6 contain a large extracellular domain (ECD) with 17 LRR modules capped at either end by N- and C-cap modules, as is typical of extracellular $\beta$-solenoid LRR proteins.[24] The LGR4−LGR6 ECDs are ~50−60% identical in amino acid sequence. The four RSPOs promiscuously bind the LGR4−LGR6 ECDs with affinities in the low nanomolar range.[15−17] Despite their homology to the G protein-coupled receptors (GPCRs) for

glycoprotein hormones such as FSH, LGR4−LGR6 do not signal through classical GPCR pathways.[15,16]

The mechanistic basis for RSPO actions became clearer with the identification of the transmembrane E3 ubiquitin ligases ZNRF3 and RNF43 as additional RSPO receptors.[25,26] ZNRF3 and RNF43 are RING-type E3 ubiquitin ligases that ubiquitinylate the 7-TM Frizzled (Fzd) receptors for Wnts, thereby promoting their degradation. Thus, ZNRF3 and RNF43 determine the availability of Fzd-LRP5/6 Wnt receptor complexes on the cell surface. ZNRF3 and RNF43 contain an ECD for RSPO binding, a single TM helix, and a cytoplasmic RING domain and C-terminal tail. RSPO-mediated association of LGRs with ZNRF3 and RNF43 results in membrane clearance of the ubiquitin ligases, thereby increasing cell surface Wnt receptor levels.[25] Interactions of RSPO with ZNRF3 and RNF43 are less well characterized than their interactions with LGR4−LGR6. The ZNRF3 and RNF43 ECDs are ∼40% identical in amino acid sequence.

Recently, four groups reported crystal structures of the RSPO1 Fu1−Fu2 fragment alone and in complex with the LGR4 or LGR5 ECDs, and a ternary RSPO1 Fu1−Fu2:LGR5 ECD:RNF43 ECD complex.[27−30] These studies revealed a disulfide- and β-hairpin-rich RSPO1 Fu1−Fu2 structure that binds to the concave surface of LGR4 and LGR5 LRR modules 3−9 via hydrophobic and charged interactions contributed by residues from both RSPO1 Fu domains. A β-hairpin loop projection in RSPO1 Fu1 interacts with a groove in the RNF43 ECD to mediate formation of the ternary complex in which RSPO1 is sandwiched between the two receptors.[27] Although the binding of RSPO2−RSPO4 to the two receptors will surely share features in common with that of RSPO1, how the different RSPOs compare in terms of their abilities to form ternary complexes remains unclear.

Previous studies of RSPOs and their receptors used recombinant proteins expressed in HEK293, CHO, or insect cells, as is common for complex disulfide-bonded glycoproteins. Here, we report a unique methodology for the bacterial expression and purification of all four human RSPO Fu1−2 domains, a fragment of the LGR4 ECD, and the ZNRF3 ECD. We characterize the activities of the proteins in a cell-based Wnt signaling assay and their interactions in biochemical binding assays. Our results provide a cost-effective source of recombinant RSPOs, introduce TR-FRET and native gel mobility shift binding assays for RSPO−receptor interactions, characterize the relative affinities of the four RSPOs for both LGR4 and ZNRF3, and demonstrate RSPO-mediated ternary complex formation with nonglycosylated proteins. Our findings provide new insights into the molecular bases for the differing signaling potencies of the four human RSPOs.

## ■ EXPERIMENTAL PROCEDURES

**Plasmids and Plasmid Construction.** cDNA plasmids for the four human R-spondins were from Origene (Rockville, MD). The pcDNA3.1/hLGR4 cDNA plasmid was from the Missouri S&T cDNA resource center. A synthetic hZNRF3 gene fragment encoding the ECD was obtained from DNA2.0 (Menlo Park, CA). The firefly luciferase reporter plasmid Super8X Topflash was from Addgene, and control renilla luciferase plasmid pRL-TK was from Promega. Bacterial protein expression plasmids were constructed with standard polymerase chain reaction-based and restriction endonuclease-based cloning methods using the parental pETDuet-1-based expression plasmids previously described.[31,32] The first multiple

cloning site encodes maltose binding protein (MBP) ending with an NAAAEF linker or, alternatively, ending with a GSSSGGGLVPRGS linker sequence for cleavage by thrombin protease. The second multiple cloning site encodes untagged *Escherichia coli* disulfide bond isomerase DsbC. Gene fragments encoding the RSPO Fu1−2 domains, LGR4 LRR1−14, and ZNRF3 ECD without their predicted signal peptides (SignalP server) and with a C-terminal $(His)_6$ tag and stop codon were amplified via polymerase chain reaction as EcoRI-NotI (for the NAAAEF linker plasmid) or BamHI-NotI (for the thrombin cleavage site plasmid) fragments, digested with the appropriate restriction enzymes, and ligated into a similarly digested expression plasmid. Primer sequences are available from the authors upon request. The coding regions of the plasmids were verified by automated DNA sequencing at The Oklahoma University Health Sciences Center Microgen core facility. The following plasmids were used (RSPO, LGR4, and ZNRF3 amino acid residue numbers are indicated; Th designates the thrombin cleavage site): pHH047, pETDuet1/MBP-RSPO1.21−145-$H_6$/DsbC; pHH048, pETDuet1/MBP-RSPO2.22−144-$H_6$/DsbC; pAP345, pETDuet1/MBP-RSPO3.22−146-$H_6$/DsbC; pAP338, pETDuet1/MBP-RSPO4.21−138-$H_6$/DsbC; pAP351, pETDuet1/MBP-Th-RSPO1.21−145-$H_6$/DsbC; pAP323, pETDuet1/MBP-LGR4.25−383-$H_6$/DsbC; pAP319, pETDuet1/MBP-Th-LGR4.23−383-$H_6$/DsbC; pAP346, pETDuet1/MBP-ZNRF3.56−216-$H_6$/DsbC; pAP353, pETDuet1/MBP-Th-ZNRF3.56−216-$H_6$/DsbC.

**Protein Expression and Purification.** Protein expression was performed in *E. coli* Origami B (DE3) *trxB gor* cells (Novagen) as previously described.[31] The culture volumes were 6 L for RSPOs and LGR4 and 3 L for ZNRF3. The inductions were conducted at 16 °C overnight with IPTG concentrations of 0.4 mM for RSPOs and ZNRF3 or 0.2 mM for LGR4. All purification steps were performed at 4 °C unless otherwise indicated, and the column chromatography steps utilized an AKTA purifier (GE Healthcare). The purification protocols for the four MBP-RSPOs and MBP-LGR4 were identical, except where noted. The cells were lysed by sonication, the lysate was clarified by centrifugation, and the soluble fusion protein was purified from the supernatant by IMAC and Amylose affinity chromatography using buffers and methods previously described.[31] The peak amylose fractions were subjected to *in vitro* disulfide shuffling in 50 mM Tris-HCl (pH 8.0), 5% (v/v) glycerol, 150 mM NaCl, and 1 mM EDTA supplemented with glutathione redox reagents. RSPO1 and -4 received 5 mM GSH, 1 mM GSSG, and RSPO2 and -3, and LGR4 received 1 mM GSH and 1 mM GSSG. The RSPO proteins were incubated at 20 °C at a protein concentration of 1 mg/mL, whereas the LGR4 proteins were incubated at 12 °C at a protein concentration of 0.4 mg/mL. After overnight disulfide shuffling, the protein was concentrated by ammonium sulfate precipitation as previously described[31] and loaded on a Superdex200 HR gel-filtration column (GE Healthcare) equilibrated in and eluted with 50 mM Tris-HCl (pH 7.5), 10% (v/v) glycerol, and 150 mM NaCl. The peak MBP-LGR4 fractions from gel filtration were dialyzed to 25 mM HEPES (pH 7.5), 50% (v/v) glycerol, and 150 mM NaCl (storage buffer) and stored at −80 °C. The four MBP-RSPO proteins were subjected to an additional anion exchange chromatography step. The peak gel-filtration fractions were dialyzed to 25 mM Tris-HCl (pH 7.5) and 10% (v/v) glycerol (Q buffer A) and loaded on a 5 mL QFF column (GE Healthcare). The

column was washed with Q buffer A and eluted with a linear gradient of Q buffer A to Q buffer A with 1 M NaCl. Peak fractions were dialyzed to storage buffer and stored at −80 °C.

The MBP fusion versions of RSPO1 and LGR4 containing the thrombin cleavage site were purified as described above through the gel-filtration step and then digested with human α-thrombin protease (HTI). MBP-Th-RSPO1 was digested at a 1:750 ratio (thrombin weight:fusion protein weight) overnight at 4 °C with dialysis to 50 mM Na/K phosphate (pH 7.0) and 5% (v/v) glycerol (S buffer A). The digested sample was applied to a 5 mL SP cation exchange column (GE Healthcare) to remove MBP and the protease. The column was washed in S buffer A, and RSPO1 was eluted with a linear gradient of S buffer A to S buffer A with 1 M NaCl. Peak RSPO1 fractions were dialyzed to storage buffer and stored at −80 °C. MBP-Th-LGR4 was digested at a 1:325 ratio overnight at 4 °C with dialysis to 50 mM Tris-HCl (pH 7.5), 2.5% (v/v) glycerol, and 150 mM NaCl. The digested sample was passed over a 1 mL amylose column by gravity flow to remove free MBP and any undigested fusion protein. The flow-through containing LGR4 and protease was applied to a 2 mL Ni-NTA agarose column (Qiagen) by gravity flow to remove protease. The eluted LGR4 protein was dialyzed to storage buffer and stored at −80 °C.

The MBP-ZNRF3 ECD purification was the same as the MBP-LGR4 purification with the exception that *in vitro* disulfide shuffling was omitted. The MBP-Th-ZNRF3 protein was purified in the same manner and digested with thrombin at a 1:300 ratio overnight at 4 °C. The digested sample was applied to a Ni column followed by gel filtration as described above. Peak ZNRF3 ECD fractions were pooled, dialyzed to storage buffer, and stored at −80 °C. Protein concentrations were determined by the Bradford assay with a BSA standard curve and are stated in terms of the monomers. Full-length recombinant hRSPO1 produced in CHO cells was purchased from R&D Systems (catalog no. 4645-RS-025CF). The concentration of the reconstituted R&D RSPO1 was determined by UV absorbance at 280 nm. RAMP2 ECD and MBP-CRFR1 ECD control proteins were previously described.[31,33]

**Native Gel Mobility Shift Assay.** Purified proteins were mixed at the indicated concentrations in a buffer of 50 mM HEPES (pH 7.5), 10% (v/v) glycerol, and 150 mM NaCl, incubated at room temperature for 1 h, and electrophoresed on a nondenaturing (native) 12% polyacrylamide gel at 4 °C. Native gel electrophoresis was performed as previously described with a pH 9.0 running buffer.[32] To identify the proteins present in a given native gel band, the gel band of interest was excised with a razor blade, placed into the well of a denaturing sodium dodecyl sulfate−polyacrylamide gel electrophoresis (SDS−PAGE) gel, and overlaid with 1× SDS loading buffer before electrophoresis by standard SDS−PAGE methods. Native and SDS gels were stained with Coomassie brilliant blue.

**Labeling Proteins for LanthaScreen TR-FRET.** MBP-LGR4 and MBP-RSPO2 proteins were labeled with LanthaScreen amine reactive terbium (Tb) chelate and Alexa-fluor488 (AF488) 5-TFPE (Invitrogen), respectively, in 500 μL reaction volumes with a 10-fold molar excess of the label over protein at concentrations of 10−35 μM in a buffer of 50 mM HEPES (pH 8.0) and 150 mM NaCl. The MBP-LGR4 and MBP-RSPO2 labeling reaction mixtures were incubated at room temperature in the dark for 3 and 2 h, respectively. The reactions were quenched with 20 mM Tris-HCl (pH 7.5), and

the labeled proteins were separated from the free label on a 2.1 mL Sephadex G-25 gel-filtration column (GE Healthcare) equilibrated in 50 mM HEPES (pH 7.5), 10% (v/v) glycerol, and 150 mM NaCl. The labeled protein concentrations and the degree of labeling were determined by UV−vis spectropho-tometry making use of the protein absorbance at 280 nm, the Tb chelate absorbance at 343 nm, and the AF488 absorbance at 494 nm, according to the manufacturer's directions. UV−vis spectra were recorded on a PolarStar Omega plate reader (BMG Labtech).

**LanthaScreen TR-FRET Assay.** Proteins were mixed as indicated in a buffer of 50 mM HEPES (pH 7.5), 150 mM NaCl, 0.3% (v/v) Triton X-100, and 7 mg/mL fatty acid-free BSA (PAA laboratories) and incubated in microfuge tubes at room temperature in the dark for 2 h. Aliquots (20 μL) of the binding reaction mixtures were transferred to the wells of a white ProxiPlate-384 Plus microplate (Perkin-Elmer) for reading in a Polarstar Omega plate reader equipped with a TR-FRET advanced optic head (BMG Labtech). The filters used were TREX excitation and 490 and 520 nm emission filters for LanthaScreen (BMG Labtech). Excitation with 100 flashes/well was followed by a 100 μs delay before 490 and 520 nm emissions were read for 200 μs. Instrument gain was set to 2400. Data analysis and nonlinear regression fitting of binding curves utilized GraphPad Prism 5.0 (GraphPad Software). The sensitized emission 520 nm data were used for all binding curve analyses. Saturation binding data were fit with a one-site saturation binding equation to fit both total and nonspecific binding to determine the $K_D$. Competition binding data were fit with a one-site competitive binding equation to determine $IC_{50}$ values. $K_I$ values were calculated with the Cheng−Prusoff correction using the $K_D$ value determined by saturation binding.

**TOPFLASH Wnt Signaling Reporter Assay.** This assay was similar to those previously described.[15−17] The HEK293T cell line was from Thermo Scientific. The mouse L-Wnt3a and control L cell lines were from ATCC. Wnt3a and control conditioned media were prepared as described in the ATCC documentation. Transient transfections were performed in 96-well tissue culture plates using the reverse transfection method with FuGENE HD transfection reagent (Promega). Plasmid DNA was mixed with FuGENE HD according to the manufacturer's instructions. Each well received 100 ng of total plasmid DNA composed of 50 ng of Super8x TOPFLASH reporter and 10 ng of pRL-TK, with the remainder consisting of empty pcDNA3.1 (40 ng) or a mixture of empty pcDNA3.1 (20 ng) and pcDNA3.1/hLGR4 (20 ng) as indicated. After addition of DNA, each well was seeded with 20000 HEK293T cells in DMEM with 10% FBS, and the plate was incubated overnight. The next day, the medium was aspirated off and replaced with diluted Wnt3a or control conditioned medium containing recombinant proteins as indicated and incubated overnight. Dilutions were in DMEM, 10% FBS, and 50 units/mL penicillin with 50 μg/mL streptomycin. The next morning, the medium was aspirated from the cells, the cells were rinsed with PBS (pH 7.4), and passive lysis buffer was added to lyse the cells in preparation for the Dual Luciferase Reporter assay (Promega), which was performed according to the manufac-turer's directions. Luminescence was recorded in white 96-well Costar plates (Corning) using a PolarStar Omega plate reader equipped with dual reagent injectors (BMG Labtech). Data analysis and nonlinear regression fitting of dose−response curves were performed with GraphPad Prism 5.0 (GraphPad Software). Stimulatory dose−response curves were fit with a
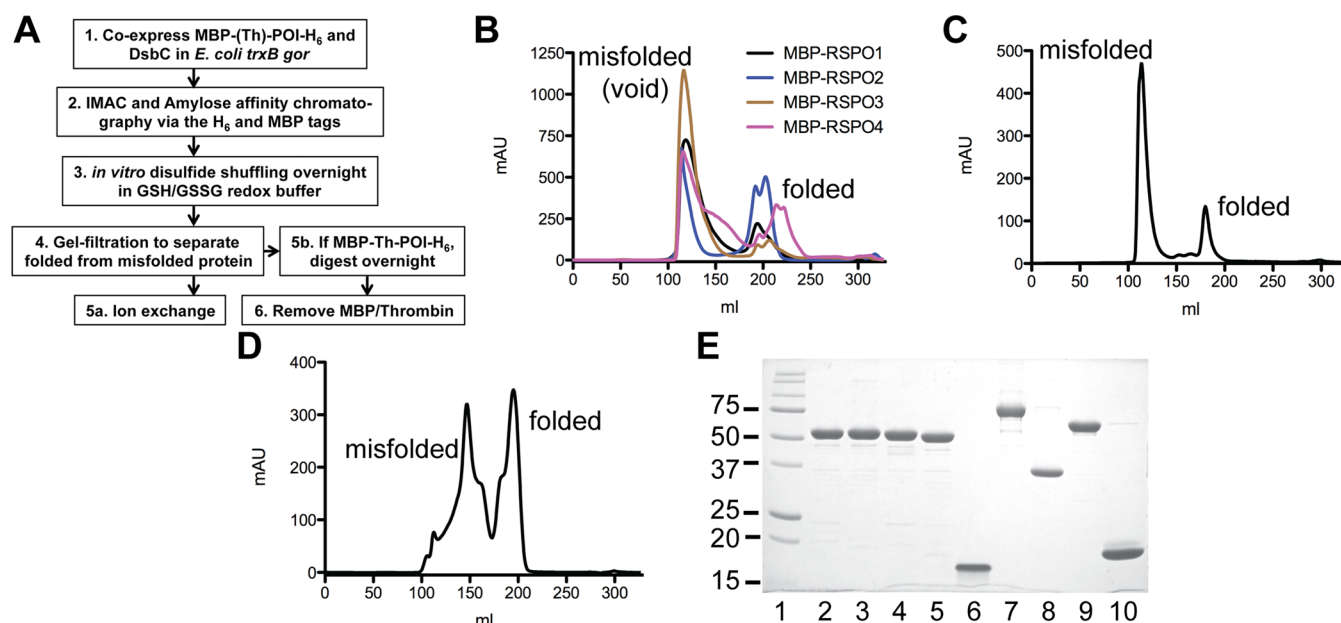
**Figure 1.** Recombinant protein production. (A) Protein expression and purification methodology. Step 5a was omitted for LGR4 LRR1−14, and steps 3 and 5a were omitted for the ZNRF3 ECD. Step 6 varied depending on the protein; for details, see Experimental Procedures. Abbreviations: (Th), optional thrombin cleavage site; POI, protein of interest. (B) Superdex200 HR gel-filtration elution profiles for the four MBP-RSPO Fu1−2 proteins. (C) Gel-filtration profile for MBP-LGR4 LRR1−14. (D) Gel-filtration profile for the MBP-ZNRF3 ECD. (E) Nonreducing SDS−PAGE analysis of the purified proteins. Molecular masses of molecular mass markers are in kilodaltons. The gel was stained with Coomassie Blue: lane 1, marker; lane 2, MBP-RSPO1; lane 3, MBP-RSPO2; lane 4, MBP-RSPO3; lane 5, MBP-RSPO4; lane 6, RSPO1; lane 7, MBP-LGR4 LRR1−14; lane 8, LGR4 LRR1−14; lane 9, MBP-ZNRF3 ECD; lane 10, ZNRF3 ECD. Each lane was loaded with 3 μg of protein.

four-parameter, variable-slope log(agonist) versus response equation. Inhibitory dose−response curves were fit with a three-parameter, fixed slope log(inhibitor) versus response equation.

## ■ RESULTS

**Bacterial Expression and Purification of Human RSPO1−RSPO4 Fu1−2 Domains, Human LGR4 LRR1− 14, and the Human ZNRF3 ECD.** We sought to apply our previously developed methodology for bacterial expression and purification of disulfide (S−S) bond-containing proteins[31,32] to the human R-spondins and LGR4 and ZNRF3 ECDs. The methodology is a hybrid approach involving *in vivo* disulfide bond formation during expression and *in vitro* "disulfide shuffling" during purification. The protein of interest (POI) is fused to the C-terminus of maltose binding protein (MBP), and the soluble MBP-POI-(His)₆ fusion protein is co-expressed with the disulfide bond isomerase DsbC in the oxidizing cytoplasm of *E. coli trxB gor*. This *in vivo* step is sometimes sufficient for proper folding of the POI,[31] but frequently, the POI is completely misfolded or is a mixture of folded and misfolded species.[31−35] Fortunately, the misfolded POI can often be rescued by *in vitro* S−S bond shuffling in glutathione redox buffer with addition of purified DsbC.[31,32] In favorable cases, the glutathione redox buffer alone is sufficient to rescue the misfolded POI.[33] MBP is crucial because it maintains the POI in a soluble form throughout the process; it can be removed later if necessary by inclusion of a protease cleavage site between MBP and the POI.[31,36] The RSPO Fu1−2 domains, LGR4 ECD, and ZNRF3 ECD contain eight S−S bonds, five S−S bonds, and one S−S bond, respectively.[27−30] Bacterial expression plasmids were constructed for the four human RSPO Fu1−2 domains, the LGR4 ECD, and the ZNRF3 ECD as MBP fusions and for the RSPO1 Fu1−2

domains, LGR4 ECD, and ZNRF3 ECD as MBP fusions containing a thrombin protease cleavage site. All constructs except the LGR4 ECD were expressed in *E. coli trxB gor* (data not shown). Fortunately, a truncated LGR4 ECD construct containing the N-cap and LRR modules 1−14 (with three S−S bonds) was expressed (data not shown), so we proceeded with this LGR4 construct.

The protein expression and purification strategy is outlined in Figure 1A. The four MBP-RSPO Fu1−2 proteins were purified by IMAC and amylose affinity chromatography followed by *in vitro* disulfide shuffling overnight in glutathione redox buffer. Addition of purified DsbC to the disulfide shuffling reaction mixtures was unnecessary (data not shown). The folded protein was separated from remaining misfolded/ aggregated material by gel-filtration chromatography (Figure 1B). The "folded" peaks from gel filtration were pooled and subjected to anion exchange chromatography, from which each of the four MBP-RSPO Fu1−2 proteins eluted as a single, symmetric peak (data not shown). Yields ranged from ∼7 mg for MBP-RSPO3 to ∼40 mg for MBP-RSPO2 from 6 L bacterial cultures. MBP-free RSPO1 Fu1−2 protein was purified in a similar manner making use of thrombin protease to remove the MBP. The final RSPO proteins were highly purified (Figure 1E, lanes 2−6).

The MBP-LGR4 LRR1−14 and MBP-ZNRF3 ECD proteins were purified similarly, except that the anion exchange step was unnecessary and ZNRF3 did not require *in vitro* disulfide shuffling, presumably because of its simple single disulfide bond composition. Both proteins yielded single "folded" peaks on gel filtration (Figure 1C,D). The yield of MBP-LGR4 LRR1−14 was ∼6 mg from a 6 L culture, and the yield of MBP-ZNRF3 ECD was ∼22 mg from a 3 L culture. MBP-free LGR4 LRR1− 14 and the ZNRF3 ECD were purified in a similar manner making use of thrombin protease to remove the MBP. The final
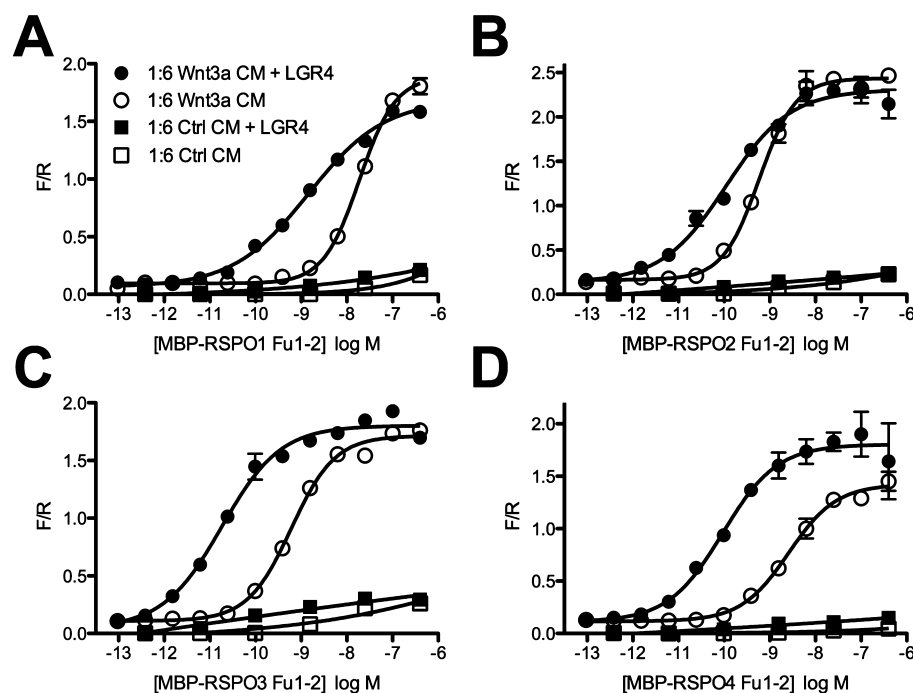
**Figure 2.** Potentiation of Wnt signaling in HEK293T cells by recombinant MBP-RSPO Fu1−2 proteins. Panels A−D are for MBP-RSPO1−RSPO4, respectively. HEK293T cells were transiently transfected with TOPFLASH Firefly luciferase reporter, Renilla luciferase control plasmid, and empty pcDNA3.1 or pcDNA3.1 expressing LGR4 (+LGR4). The transfected cells were stimulated with the indicated concentrations of the recombinant proteins in 1:6 diluted Wnt3a or control conditioned medium (CM). Data are averages of duplicate samples and are plotted as the Firefly luciferase activity/Renilla luciferase activity (F/R) ratio. The $EC_{50}$ values for MBP-RSPO1−RSPO4 in the absence of overexpressed LGR4 were 19, 0.59, 0.61, and 3 nM, respectively.

LGR4 and ZNRF3 proteins were highly purified (Figure 1E, lanes 7−10). Notably, we could also obtain properly folded MBP-LGR4 LRR1−14, and even MBP-RSPO1 and -RSPO2 Fu1−2 proteins, with omission of the *in vitro* disulfide shuffling step, but the yields were approximately half of those obtained when disulfide shuffling was included (data not shown).

The oligomeric states of the MBP fusion proteins were assessed from their gel-filtration elution volumes via comparison to a standard curve (data not shown). MBP-RSPO1 Fu1−2, MBP-LGR4 LRR1−14, and the MBP-ZNRF3 ECD eluted at volumes corresponding to molecular masses of 63, 91, and 60 kDa, respectively, which were consistent with the calculated monomer molecular masses. In contrast, MBP-RSPO2−RSPO4 Fu1−2 proteins each exhibited a small gel-filtration peak at the position corresponding to the monomer (∼60 kDa) and larger peaks at positions corresponding to molecular masses of 48, 44, and 35 kDa, respectively (Figure 1B). We saw no evidence of proteolytic degradation (Figure 1E, lanes 3−5). The MBP-RSPO2−RSPO4 proteins may have some affinity for the gel-filtration resin that caused delayed elution. Thus, all four RSPOs, LGR4 LRR1−14, and the ZNRF3 ECD appeared to be monomeric.

**Pharmacological Characterization of the Recombinant Proteins in a HEK293T Cell-Based Wnt Signaling Assay.** The four purified MBP-RSPO Fu1−2 proteins enhanced low-dose Wnt3a activation of the Wnt/$\beta$-catenin pathway in a HEK293T cell-based TOPFLASH reporter assay, and the activities of the fusion proteins were further increased by overexpression of LGR4 in the cells (Figure 2A−D). MBP-RSPO1−RSPO4 exhibited $EC_{50}$ values of 19, 0.59, 0.61, and 3 nM, respectively, in the absence of overexpressed LGR4. Thus, the signaling potency rank order was as follows: MBP-RSPO2

and -RSPO3 > MBP-RSPO4 > MBP-RSPO1. The observed potencies of the MBP-RSPO fusion proteins were comparable to those reported for full-length RSPO proteins produced in mammalian cells, and our observed rank order of potencies was consistent with previous reports that RSPO2 and -3 were more potent than RSPO1 and -4.[15,37] Direct comparison of our MBP-RSPO1 Fu1−2 and RSPO1 Fu1−2 proteins with commercially available full-length RSPO1 produced in CHO cells indicated that the bacterially produced proteins exhibited potencies comparable, albeit not quite equal, to that of the commercial product (Figure 3). These results suggested that
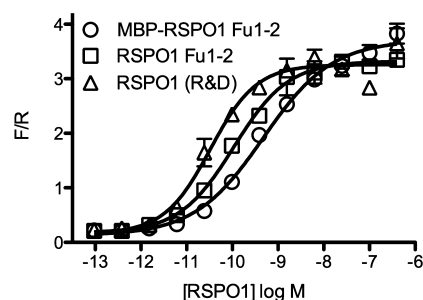


**Figure 3.** Signaling potencies of recombinant RSPO1 Fu1−2 proteins produced in *E. coli* compared with that of commercially available recombinant RSPO1 produced in CHO cells. HEK293T cells were transiently transfected with TOPFLASH Firefly luciferase reporter, Renilla luciferase control plasmid, and pcDNA3.1 expressing LGR4. The cells were stimulated with the indicated concentrations of MBP-RSPO1 Fu1−2, RSPO Fu1−2 (no MBP), or R&D systems RSPO1 in 1:6 diluted Wnt3a conditioned medium. Data are averages of duplicate samples and are plotted as the Firefly luciferase activity/Renilla luciferase activity (F/R) ratio.
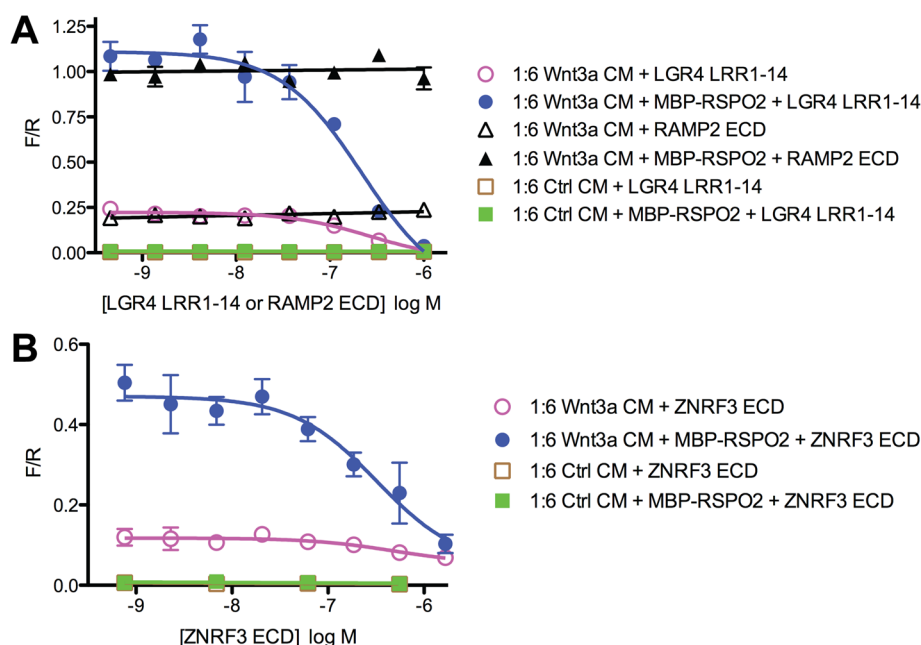
**Figure 4.** Inhibition of RSPO-enhanced Wnt signaling in HEK293T cells by recombinant LGR4 LRR1−14 and the ZNRF3 ECD. HEK293T cells were transiently transfected with TOPFLASH Firefly luciferase reporter, Renilla luciferase control plasmid, and empty pcDNA3.1. The cells were treated with the indicated concentrations of control RAMP2 ECD, LGR4 LRR1−14, or ZNRF3 ECD protein in 1:6 diluted Wnt3a or control conditioned medium (CM) in the absence or presence of MBP-RSPO2 Fu1−2 (200 pM). Data are averages of duplicate samples and are plotted as the Firefly luciferase activity/Renilla luciferase activity (F/R) ratio. (A) Inhibition by LGR4 LRR1−14. The IC$_{50}$ values for LGR4 LRR1−14 in the absence and presence of MBP-RSPO2 were 270 and 220 nM, respectively. (B) Inhibition by the ZNRF3 ECD. The IC$_{50}$ value for the ZNRF3 ECD in the presence of MBP-RSPO2 was 440 nM.

the MBP tag did not significantly alter RSPO function and indicated that our RSPO proteins were comparable to those produced in mammalian cells with respect to their ability to potentiate Wnt signaling.

Purified LGR4 LRR1−14 inhibited MBP-RSPO2-enhanced Wnt3a signaling with an IC$_{50}$ value of 220 nM, presumably by sequestering MBP-RSPO2 (Figure 4A). As a control for specificity, we tested the ECD of receptor activity modifying protein 2 (RAMP2), which is not known to be involved in Wnt signaling but was produced in *E. coli* using a similar expression and purification methodology.[31] The RAMP2 ECD had no effect in the assay as expected (Figure 4A). Interestingly, LGR4 LRR1−14 also inhibited signaling in the absence of exogenous RSPO2 (Figure 4A), possibly by blocking autocrine RSPO signaling because HEK293T cells express RSPOs.[5] We further tested the ability of LGR4 LRR1−14 to inhibit signaling induced by a larger Wnt3a dose and observed a similar inhibition of signaling (Figure S1 of the Supporting Information). The purified ZNRF3 ECD also inhibited MBP-RSPO2-enhanced Wnt signaling, although with a potency (IC$_{50}$ = 440 nM) reduced compared to that of LGR4 LRR1−14 (Figure 4B). These results indicated that both LGR4 LRR1−14 and the ZNRF3 ECD function as inhibitors of RSPO-enhanced Wnt3a signaling in HEK293T cells, whereas LGR4 LRR1−14 also appeared to act as an inhibitor of Wnt3a signaling. The results further suggested that the ZNRF3 ECD binds RSPOs with a lower affinity than the LGR4 ECD.

**Quantitative TR-FRET Assay for Assessing Binary RSPO−LGR4 Interactions *in Vitro*.** A LanthaScreen (Invitrogen) time-resolved fluorescence resonance energy transfer (TR-FRET) assay was developed for measuring interactions between RSPO Fu1−2 and LGR4 LRR1−14. The TR-FRET technology is well-suited for affinities in the expected

nanomolar range. MBP-LGR4 LRR1−14 and MBP-RSPO2 Fu1−2 proteins were nonspecifically labeled with a terbium chelate donor and AlexaFluor488 acceptor, respectively, via amine reactive chemistry. Quantitation of the labeling efficiencies indicated one Tb label per MBP-LGR4 LRR1−14 molecule and two AF488 labels per MBP-RSPO2 Fu1−2 molecule (data not shown). The labeled MBP-RSPO2 Fu1−2 retained normal activity in the Wnt signaling assay (Figure S2 of the Supporting Information) and bound the labeled MBP-LGR4 LRR1−14 with a $K_D$ of 120 nM in a saturation binding assay (Figure 5A). The binding of the four unlabeled MBP-RSPO Fu1−2 proteins was assessed in a competition binding assay. MBP-RSPO1−RSPO4 displaced the binding of labeled MBP-RSPO2 with $K_I$ values of 380, 37, 100, and 14 nM, respectively (Figure 5B). Competition assays comparing the MBP fusion and MBP-free versions of RSPO1 Fu1−2 and LGR4 LRR1−14 indicated that the MBP tags did not significantly alter the protein−protein interactions (Figure S3A,B of the Supporting Information).

**Native Gel Mobility Shift Assays for Binary RSPO−Receptor Complexes.** The MBP-RSPO fusion proteins afforded us the opportunity to develop a simple and rapid assay for RSPO−receptor interactions based on native gel electrophoretic mobility shifts. The basic pI values of the RSPOs would cause them to migrate in native gel electrophoresis in the opposite direction of the LGR4 and ZNRF3 ECDs, which have acidic pI values. Fortunately, MBP sufficiently lowers the overall pI values of the MBP-RSPO proteins to allow the use of native gel electrophoresis to monitor complex formation. Binary complexes with MBP-LGR4 LRR1−14 were detected for all four MBP-RSPO Fu1−2 proteins as distinct shifted bands of slower mobility on native gels (Figure 6A−D). The MBP-RSPO and MBP-LGR4 bands
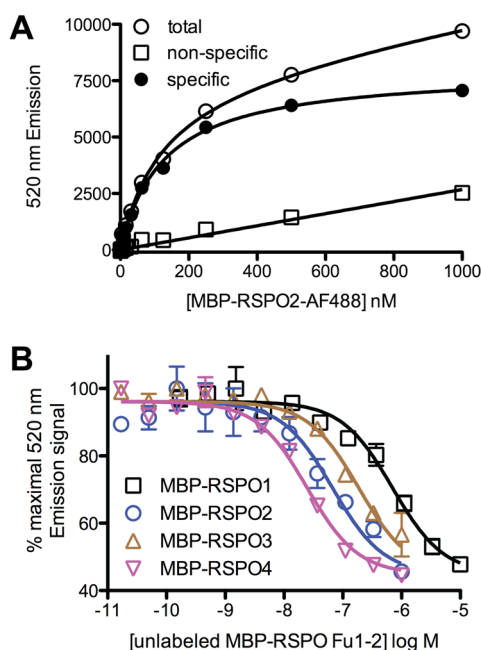
**Figure 5.** Quantitative TR-FRET binding assay for binary interactions between MBP-RSPO and MBP-LGR4 LRR1−14. (A) Saturation binding. Tb chelate-labeled MBP-LGR4 LRR1−14 (10 nM) was incubated with the indicated concentrations of AF488-labeled MBP-RSPO2 Fu1−2 in the absence (total) or presence (nonspecific) of unlabeled MBP-RSPO4 Fu1−2 (40 $\mu$M). Nonlinear regression yielded a $K_D$ value of 120 nM. (B) Competition binding. Tb chelate-labeled MBP-LGR4 LRR1−14 (10 nM) and AF488-labeled MBP-RSPO2 Fu1−2 (100 nM) were incubated with the indicated concentrations of unlabeled MBP-RSPO proteins. Nonlinear regression yielded $K_I$ values of 380, 37, 100, and 14 nM for MBP-RSPO1−RSPO4, respectively. Data shown in both panels are averages of duplicate samples. Error bars are smaller than the symbols in many cases.
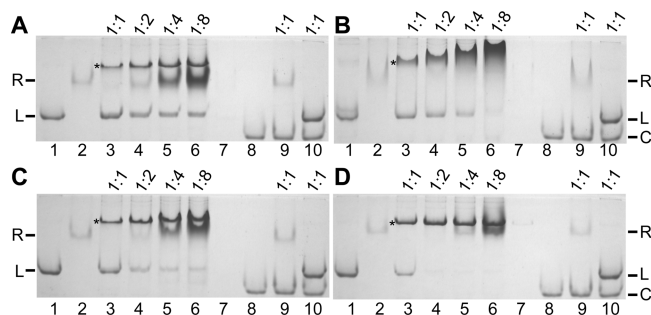


**Figure 6.** Native gel mobility shift assays with MBP-RSPOs and MBP-LGR4 LRR1−14. Panels A−D are for MBP-RSPO1−RSPO4, respectively: lane 1, MBP-LGR4 alone (1 $\mu$M); lane 2, MBP-RSPO alone (1 $\mu$M); lanes 3−6, MBP-RSPO with MBP-LGR4 at the indicated MBP-LGR4:MBP-RSPO ratios (in micromolar); lane 7, empty; lane 8, MBP-CRFR1 ECD alone (1 $\mu$M); lane 9, MBP-RSPO with MBP-CRFR1 ECD (1 $\mu$M each); lane 10, MBP-LGR4 with MBP-CRFR1 ECD (1 $\mu$M each). The protein bands are indicated as follows: L, MBP-LGR4 LRR1−14; R, MBP-RSPO Fu1−2; C, MBP-CRFR1 ECD. The asterisk highlights the binary complex bands. The gels were stained with Coomassie Blue.

were not altered in the presence of a control MBP-CRFR1 ECD protein,[33] which indicated specificity. Comparing the disappearance of the MBP-LGR4 band with the increasing MBP-RSPO concentration among the panels in Figure 6 corroborated the TR-FRET data that the affinity rank order was

as follows: RSPO4 > RSPO2 > RSPO3 > RSPO1. MBP-RSPO2 was unique because increasing its concentration yielded further shifts in mobility (Figure 6B). However, the MBP-RSPO2 protein alone exhibited the same behavior (Figure S4 of the Supporting Information), so the slowing mobility with an increasing MBP-RSPO2 concentration in Figure 6B did not appear to reflect formation of higher-order complexes of MBP-RSPO2 and MBP-LGR4 LRR1−14. The native gel results suggested that a substantial fraction of the protein in our purified protein samples was functional because essentially all of the visible protein could be shifted into the complex bands. Similar results were observed using the MBP-free LGR4 LRR1−14 protein, except that the binary complexes exhibited mobilities that were faster than those of the MBP-RSPO proteins alone (Figure S5 of the Supporting Information, and see Figure 8), presumably because of alterations in charge upon complex formation.

We further used the native gel assay to assess interactions of MBP-RSPO with the MBP-ZNRF3 ECD (Figure 7). Binary
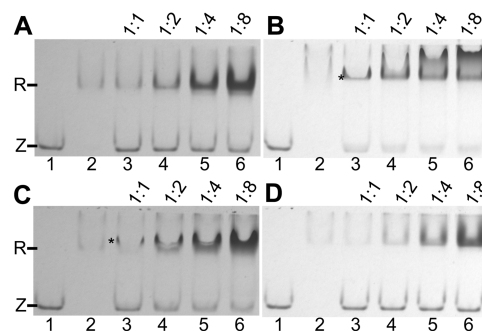


**Figure 7.** Native gel mobility shift assays with MBP-RSPOs and MBP-ZNRF3 ECD. Panels A−D are for MBP-RSPO1−RSPO4, respectively: lane 1, MBP-ZNRF3 ECD alone (1 $\mu$M); lane 2, MBP-RSPO alone (1 $\mu$M); lanes 3−6, MBP-RSPO with MBP-ZNRF3 at the indicated MBP-ZNRF3:MBP-RSPO ratios (in micromolar). The protein bands are indicated as follows: Z, MBP-ZNRF3 ECD; R, MBP-RSPO Fu1−2. The asterisk highlights the binary complex bands. The gels were stained with Coomassie Blue.

complexes were detected as distinct bands with slower mobility for MBP-RSPO2 (Figure 7B) and MBP-RSPO3 (Figure 7C). MBP-RSPO1 appeared to form weak interactions with the MBP-ZNRF3 ECD based on the slight decrease in the magnitude of the MBP-ZNRF3 ECD band with an increasing MBP-RSPO1 concentration (Figure 7A). We saw no evidence of interactions between MBP-RSPO4 and MBP-ZNRF3 (Figure 7D). The same pattern was observed using the MBP-free ZNRF3 ECD protein (Figure S6 of the Supporting Information, and see Figure 8), which suggested that the MBP tag did not significantly alter ZNRF3 ECD function. To prove the interactions of MBP-RSPO1−RSPO3 with the ZNRF3 ECD, the putative native gel complex bands were excised and analyzed by denaturing SDS−PAGE, which showed the presence of both proteins (Figure S6 of the Supporting Information, and see Figure 8). Taken together, these results indicated that the RSPOs bound the ZNRF3 ECD with the following affinity rank order: RSPO2 > RSPO3 > RSPO1. The results also suggested that RSPO-ZNRF3 interactions are weaker than RSPO-LGR4 interactions.

**Native Gel Mobility Shift Assays for Ternary RSPO−Receptor Complexes.** Ternary complex formation was
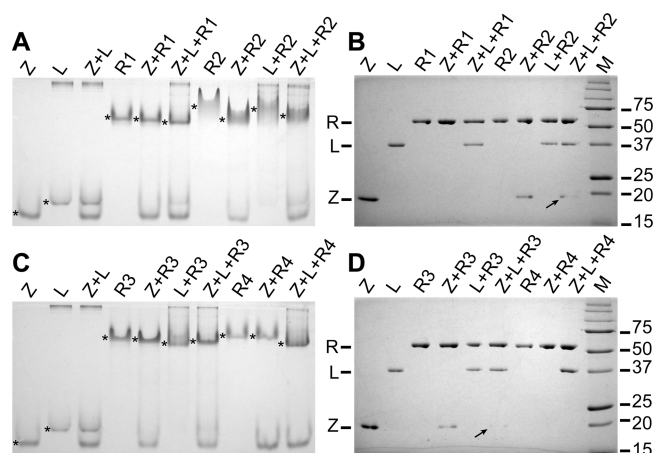
**Figure 8.** Native gel mobility shift assays with MBP-RSPOs, LGR4 LRR1−14 (no MBP), and the ZNRF3 ECD (no MBP). (A) Native gel for MBP-RSPO1 and -RSPO2. (B) Nonreducing SDS−PAGE analysis of cut out native gel bands from panel A. (C) Native gel for MBP-RSPO3 and -RSPO4. (D) Nonreducing SDS−PAGE analysis of cut out native gel bands from panel C. The protein components in each native gel lane are indicated as follows: Z, ZNRF3 ECD; L, LGR4 LRR1−14; R1−R4, MBP-RSPO1−RSPO4, respectively. Each protein was at a concentration of 2.5 $\mu$M. The asterisk to the left of the native gel bands marks the band that was cut out and analyzed by SDS−PAGE in the adjacent panel. Autocontrast was applied to the panel B and D gel images to allow better visualization of the faint ZNRF3 bands, which are highlighted by arrows for the ternary complexes. Molecular mass markers are indicated in kilodaltons. The gels were stained with Coomassie Blue.

assessed with the native gel assay using the MBP-free LGR4 LRR1−14 and ZNRF3 ECD proteins to avoid the possibility of steric hindrance with three MBP tags (Figure 8). Binary RSPO−receptor complex formation was also assessed for completeness and to allow comparison of band mobilities within the same gel. The putative binary and ternary complex native gel bands (Figure 8A,C) were excised and subjected to denaturing SDS−PAGE (Figure 8B,D) to confirm the identities of the proteins present in the native gel bands. Binary complexes with LGR4 LRR1−14 were detected for all four MBP-RSPOs, and binary complexes with the ZNRF3 ECD were detected for MBP-RSPO2 and -RSPO3, as expected. There was no evidence of binary complexes of LGR4 LRR1−14 and the ZNRF3 ECD, but ternary complexes were formed in the presence of MBP-RSPO2 or -RSPO3 (Figure 8). We did not detect ternary complexes with MBP-RSPO1 and -RSPO4, which probably reflected the poor binding of these proteins to ZNRF3. These results are consistent with RSPOs simultaneously binding both receptors to mediate ternary complex formation.

## ■ DISCUSSION

R-Spondins and their receptors, LGR4−LGR6 and ZNRF3/RNF43, are central molecules in stem cell biology. RSPOs are valuable for regenerative medicine applications, and therapeutic modulation of RSPO−receptor interactions holds potential for treating diseases such as cancer. Here, we reported a bacterial expression and purification methodology that allowed the routine production of large quantities of the signaling competent Fu1−2 domains of the four human RSPOs and the LGR4 and ZNRF3 ECDs. We characterized the signaling

activities and interactions of the proteins, culminating with the reconstitution of ternary complexes.

The RSPO Fu1−2 domains were challenging targets for bacterial expression because they contain eight disulfide bonds.[27−30] Nonetheless, our hybrid methodology utilizing co-expression of MBP-RSPO Fu1−2 fusion proteins with DsbC in *E. coli trxB gor* and *in vitro* disulfide shuffling in glutathione redox buffer allowed us to obtain significant quantities of properly folded protein for all four RSPOs (Figure 1A,B). The evidence that the proteins were properly folded included their enhancement of low-dose Wnt3a signaling with potencies comparable to those of RSPOs produced in mammalian cells (Figures 2 and 3) and their binding to LGR4 with nanomolar affinities (Figure 5), consistent with previous reports.[15−17] In addition, MBP-RSPO1, -RSPO3, and -RSPO4 exhibited distinct bands on native gels, indicative of homogeneous samples. MBP-RSPO2 exhibited a smeared band, but this may reflect an unusual property of this protein rather than misfolding. The native gel mobility shift assays further suggested that a substantial fraction, if not all, of the MBP-RSPO protein in our preps was active because it could all be shifted (Figures 6−8).

Our hybrid methodology was also successful for the LGR4 LRR1−14 with three disulfide bonds, and ZNRF3 ECD production was even simpler, presumably because it has only one disulfide bond (Figure 1C,D). The evidence that the receptor ECDs were properly folded included their inhibition of RSPO-enhanced Wnt signaling (Figure 4), their binding of the RSPOs (Figures 5−8), and their homogeneous behavior on native gels (Figures 6−8). We presume that the molecular basis for LGR4 LRR1−14 and ZNRF3 ECD inhibition of MBP-RSPO2-enhanced Wnt signaling was sequestration of the RSPO, which thereby prevented its binding to the plasma membrane-resident RSPO receptors. The LGR4 LRR1−14 inhibition of Wnt3a signaling in the absence of exogenous RSPO protein suggested that in HEK293T cells some basal level of autocrine RSPO signaling is required for Fzd-LRP5/6 Wnt receptor complexes to be present on the cell surface, which is consistent with previous reports that HEK293T cells express RSPOs and that siRNA-mediated knockdown of LGR4 or LGR5 inhibited Wnt3a signaling even in the absence of exogenous RSPOs.[5,17] However, it has also been reported that siRNA-mediated knockdown of LGR4 did not affect Wnt3a signaling in the absence of exogenous RSPOs,[16] so other mechanisms for LGR4 LRR1−14 inhibition of Wnt signaling are possible.

Binary and ternary interactions between all four RSPOs and the receptor ECDs were characterized with TR-FRET and native gel mobility shift assays (Figures 5−8), which yielded several results of note. First, all four RSPOs bound LGR4 with somewhat similar affinities in the low nanomolar range. Nonetheless, a clear rank order of affinities was observed, with RSPO4 having the highest, RSPO1 the lowest, and RSPO2 and -3 intermediate affinities for LGR4. Second, although we did not determine $K_D$ values of RSPO for ZNRF3, the native gel results clearly showed that RSPO−ZNRF3 interactions were weaker than RSPO−LGR4 interactions. These results are consistent with a recent report of the RNF43 ECD binding RSPO1 with micromolar affinity as measured by ITC.[27] We observed a clear rank order of RSPO affinities for ZNRF3 with RSPO2 and -3 binding ZNRF3 stronger than RSPO1. Our inability to detect binding of RSPO4 to ZNRF3 was probably due to an affinity below the detection limit of the native gel

assay. It seems unlikely that RSPO4 fails to bind ZNRF3 because loss-of-function mutations in RSPO4 map to the Fu1 β-hairpin loop projection that interacts with RNF43.[27] Third, ternary complexes were observed with RSPO2 and -3. Our inability to detect ternary complexes with RSPO1 and -4 likely reflected their weak ZNRF3 binding. LGR4 and ZNRF3 failed to interact in the absence of RSPOs; thus, our data are consistent with RSPOs mediating ternary complex formation by simultaneously binding both receptors. These results are in agreement with and complement the crystal structure of the ternary complex of RSPO1 Fu1−2, the LGR5 ECD, and the RNF43 ECD.[27] One difference between the study reporting the structure of the ternary complex and our data is that in the structural study it was reported that the affinity of RSPO1 for the RNF43 ECD was increased in the presence of the LGR5 ECD,[27] whereas in our native gel assays, MBP-RSPO2 and -3 appeared to bind the ZNRF3 ECD somewhat weaker in the ternary complexes than in the binary complexes of MBP-RSPO2- or -3 with the ZNRF3 ECD (Figure 8B,D). This apparent discrepancy might be due to our use of the MBP-RSPO fusion proteins. Although the presence of the MBP tag did not appear to significantly alter the function of the RSPOs, it may have a slight steric effect in the ternary complexes, which could also explain the slightly lower signaling potency of MBP-RSPO1 Fu1−2 compared to that of MBP-free RSPO1 Fu1−2 (Figure 3).

The receptor binding assay results provide an explanation for the differing RSPO potencies observed in the Wnt signaling assay (Figure 2). Comparison of the binding and signaling assays is reasonable because LGR4 and ZNRF3 are the predominant RSPO receptors expressed in HEK293T cells.[15,16,25,26] RSPO2 and -3 were most potent in the signaling assay, which is consistent with RSPO2 and -3 being most competent for ternary complex formation (Figure 8) as a result of their binding both LGR4 and ZNRF3 relatively well. RSPO1 exhibited the lowest signaling potency, which is consistent with its weaker binding of both receptors. RSPO4 exhibited the strongest LGR4 affinity, but the weakest ZNRF3 affinity, which is likely responsible for its intermediate signaling potency. Thus, our binding and signaling assays are entirely consistent, and taken together, they suggest that RSPO signaling potency is determined by the ability of the RSPO to form the ternary complex. The recent structural advances[27−30] should allow future studies that examine the structural bases for the differences in receptor binding affinities and signaling potencies among the four RSPOs in detail.

In summary, the results presented here provide a cost- and time-efficient methodology for recombinant RSPO production, which may find practical applications in regenerative medicine. In addition, our pharmacological and biochemical character-ization of the recombinant proteins indicated that the nonglycosylated proteins were functional, demonstrated a clear rank order of affinities of the four RSPOs for the receptors that explained their differing potencies in the Wnt signaling assay, and demonstrated ternary complex formation mediated by RSPOs. Our results may inform the development of engineered RSPOs with optimized potencies for regenerative medicine applications as well as therapeutic agents targeting the receptors.

## ■ ASSOCIATED CONTENT

### ⓈSupporting Information

Inhibition of high-dose Wnt3a signaling by LGR4 LRR1−14, signaling activity of AF488-labeled MBP-RSPO2, controls for TR-FRET experiments to assess effects of MBP, native gel control for MBP-RSPO2 alone, and native gel shift assays for the four MBP-RSPOs with MBP-free LGR4 LRR1−14 and the ZNRF3 ECD. This material is available free of charge via the Internet at http://pubs.acs.org.

## ■ AUTHOR INFORMATION

### Corresponding Author

*Department of Biochemistry and Molecular Biology, The University of Oklahoma Health Sciences Center, 975 N.E. 10th St., Oklahoma City, OK 73104. E-mail: augen-pioszak@ouhsc.edu. Telephone: (405) 271-2401. Fax: (405) 271-3910.

### Notes

The authors declare no competing financial interest.

## ■ ACKNOWLEDGMENTS

## ■ ABBREVIATIONS

RSPO, R-spondin; LRR, leucine-rich repeat; ECD, extracellular domain; 7-TM, seven-transmembrane; Fu, furin-like domain; Fzd, frizzled 7-TM receptors for Wnts; LRP, lipoprotein receptor-related protein coreceptor for Wnts; MBP, maltose binding protein; Th, thrombin cleavage site; DsbC, *E. coli* disulfide bond isomerase; POI, protein of interest; IMAC, immobilized metal affinity chromatography; GSH, reduced glutathione; GSSG, oxidized glutathione; TR-FRET, time-resolved fluorescence resonance energy transfer; AF488, AlexaFluor488.

## ■ REFERENCES

(1) de Lau, W. B., Snel, B., and Clevers, H. C. (2012) The R-spondin protein family. *Genome Biol. 13*, 242.

(2) Jin, Y. R., and Yoon, J. K. (2012) The R-spondin family of proteins: Emerging regulators of WNT signaling. *Int. J. Biochem. Cell Biol. 44*, 2278−2287.

(3) Kamata, T., Katsube, K., Michikawa, M., Yamada, M., Takada, S., and Mizusawa, H. (2004) R-spondin, a novel gene with thrombospondin type 1 domain, was expressed in the dorsal neural tube and affected in Wnts mutants. *Biochim. Biophys. Acta 1676*, 51−62.

(4) Schuijers, J., and Clevers, H. (2012) Adult mammalian stem cells: The role of Wnt, Lgr5 and R-spondins. *EMBO J. 31*, 2685−2696.

(5) Kazanskaya, O., Glinka, A., del Barco Barrantes, I., Stannek, P., Niehrs, C., and Wu, W. (2004) R-Spondin2 is a secreted activator of Wnt/β-catenin signaling and is required for *Xenopus* myogenesis. *Dev. Cell 7*, 525−534.

(6) Kim, K. A., Kakitani, M., Zhao, J., Oshima, T., Tang, T., Binnerts, M., Liu, Y., Boyle, B., Park, E., Emtage, P., Funk, W. D., and Tomizuka, K. (2005) Mitogenic influence of human R-spondin1 on the intestinal epithelium. *Science 309*, 1256−1259.

(7) Ootani, A., Li, X., Sangiorgi, E., Ho, Q. T., Ueno, H., Toda, S., Sugihara, H., Fujimoto, K., Weissman, I. L., Capecchi, M. R., and Kuo,

C. J. (2009) Sustained in vitro intestinal epithelial culture within a Wnt-dependent stem cell niche. *Nat. Med. 15*, 701−706.

(8) Sato, T., Vries, R. G., Snippert, H. J., van de Wetering, M., Barker, N., Stange, D. E., van Es, J. H., Abo, A., Kujala, P., Peters, P. J., and Clevers, H. (2009) Single Lgr5 stem cells build crypt-villus structures in vitro without a mesenchymal niche. *Nature 459*, 262−265.

(9) Sato, T., and Clevers, H. (2013) Growing self-organizing mini-guts from a single intestinal stem cell: Mechanism and applications. *Science 340*, 1190−1194.

(10) Seshagiri, S., Stawiski, E. W., Durinck, S., Modrusan, Z., Storm, E. E., Conboy, C. B., Chaudhuri, S., Guan, Y., Janakiraman, V., Jaiswal, B. S., Guillory, J., Ha, C., Dijkgraaf, G. J., Stinson, J., Gnad, F., Huntley, M. A., Degenhardt, J. D., Haverty, P. M., Bourgon, R., Wang, W., Koeppen, H., Gentleman, R., Starr, T. K., Zhang, Z., Largaespada, D. A., Wu, T. D., and de Sauvage, F. J. (2012) Recurrent R-spondin fusions in colon cancer. *Nature 488*, 660−664.

(11) Parma, P., Radi, O., Vidal, V., Chaboissier, M. C., Dellambra, E., Valentini, S., Guerra, L., Schedl, A., and Camerino, G. (2006) R-spondin1 is essential in sex determination, skin differentiation and malignancy. *Nat. Genet. 38*, 1304−1309.

(12) Blaydon, D. C., Ishii, Y., O'Toole, E. A., Unsworth, H. C., Teh, M. T., Ruschendorf, F., Sinclair, C., Hopsu-Havu, V. K., Tidman, N., Moss, C., Watson, R., de Berker, D., Wajid, M., Christiano, A. M., and Kelsell, D. P. (2006) The gene encoding R-spondin 4 (RSPO4), a secreted protein implicated in Wnt signaling, is mutated in inherited anonychia. *Nat. Genet. 38*, 1245−1247.

(13) Bruchle, N. O., Frank, J., Frank, V., Senderek, J., Akar, A., Koc, E., Rigopoulos, D., van Steensel, M., Zerres, K., and Bergmann, C. (2008) RSPO4 is the major gene in autosomal-recessive anonychia and mutations cluster in the furin-like cysteine-rich domains of the Wnt signaling ligand R-spondin 4. *J. Invest. Dermatol. 128*, 791−796.

(14) Ishii, Y., Wajid, M., Bazzi, H., Fantauzzo, K. A., Barber, A. G., Blaydon, D. C., Nam, J. S., Yoon, J. K., Kelsell, D. P., and Christiano, A. M. (2008) Mutations in R-spondin 4 (RSPO4) underlie inherited anonychia. *J. Invest. Dermatol. 128*, 867−870.

(15) Carmon, K. S., Gong, X., Lin, Q., Thomas, A., and Liu, Q. (2011) R-spondins function as ligands of the orphan receptors LGR4 and LGR5 to regulate Wnt/β-catenin signaling. *Proc. Natl. Acad. Sci. U.S.A. 108*, 11452−11457.

(16) de Lau, W., Barker, N., Low, T. Y., Koo, B. K., Li, V. S., Teunissen, H., Kujala, P., Haegebarth, A., Peters, P. J., van de Wetering, M., Stange, D. E., van Es, J. E., Guardavaccaro, D., Schasfoort, R. B., Mohri, Y., Nishimori, K., Mohammed, S., Heck, A. J., and Clevers, H. (2011) Lgr5 homologues associate with Wnt receptors and mediate R-spondin signalling. *Nature 476*, 293−297.

(17) Glinka, A., Dolde, C., Kirsch, N., Huang, Y. L., Kazanskaya, O., Ingelfinger, D., Boutros, M., Cruciat, C. M., and Niehrs, C. (2011) LGR4 and LGR5 are R-spondin receptors mediating Wnt/β-catenin and Wnt/PCP signalling. *EMBO Rep. 12*, 1055−1061.

(18) Ruffner, H., Sprunger, J., Charlat, O., Leighton-Davies, J., Grosshans, B., Salathe, A., Zietzling, S., Beck, V., Therier, M., Isken, A., Xie, Y., Zhang, Y., Hao, H., Shi, X., Liu, D., Song, Q., Clay, I., Hintzen, G., Tchorz, J., Bouchez, L. C., Michaud, G., Finan, P., Myer, V. E., Bouwmeester, T., Porter, J., Hild, M., Bassilana, F., Parker, C. N., and Cong, F. (2012) R-Spondin potentiates Wnt/β-catenin signaling through orphan receptors LGR4 and LGR5. *PLoS One 7*, e40976.

(19) Barker, N., and Clevers, H. (2010) Leucine-rich repeat-containing G-protein-coupled receptors as markers of adult stem cells. *Gastroenterology 138*, 1681−1696.

(20) Barker, N., van Es, J. H., Kuipers, J., Kujala, P., van den Born, M., Cozijnsen, M., Haegebarth, A., Korving, J., Begthel, H., Peters, P. J., and Clevers, H. (2007) Identification of stem cells in small intestine and colon by marker gene Lgr5. *Nature 449*, 1003−1007.

(21) Huch, M., Dorrell, C., Boj, S. F., van Es, J. H., Li, V. S., van de Wetering, M., Sato, T., Hamer, K., Sasaki, N., Finegold, M. J., Haft, A., Vries, R. G., Grompe, M., and Clevers, H. (2013) In vitro expansion of single Lgr5+ liver stem cells induced by Wnt-driven regeneration. *Nature 494*, 247−250.

(22) Jaks, V., Barker, N., Kasper, M., van Es, J. H., Snippert, H. J., Clevers, H., and Toftgard, R. (2008) Lgr5 marks cycling, yet long-lived, hair follicle stem cells. *Nat. Genet. 40*, 1291−1299.

(23) Snippert, H. J., Haegebarth, A., Kasper, M., Jaks, V., van Es, J. H., Barker, N., van de Wetering, M., van den Born, M., Begthel, H., Vries, R. G., Stange, D. E., Toftgard, R., and Clevers, H. (2010) Lgr6 marks stem cells in the hair follicle that generate all cell lineages of the skin. *Science 327*, 1385−1389.

(24) Bella, J., Hindle, K. L., McEwan, P. A., and Lovell, S. C. (2008) The leucine-rich repeat structure. *Cell. Mol. Life Sci. 65*, 2307−2333.

(25) Hao, H. X., Xie, Y., Zhang, Y., Charlat, O., Oster, E., Avello, M., Lei, H., Mickanin, C., Liu, D., Ruffner, H., Mao, X., Ma, Q., Zamponi, R., Bouwmeester, T., Finan, P. M., Kirschner, M. W., Porter, J. A., Serluca, F. C., and Cong, F. (2012) ZNRF3 promotes Wnt receptor turnover in an R-spondin-sensitive manner. *Nature 485*, 195−200.

(26) Koo, B. K., Spit, M., Jordens, I., Low, T. Y., Stange, D. E., van de Wetering, M., van Es, J. H., aMohammed, S., Heck, A. J., Maurice, M. M., and Clevers, H. (2012) Tumour suppressor RNF43 is a stem-cell E3 ligase that induces endocytosis of Wnt receptors. *Nature 488*, 665−669.

(27) Chen, P. H., Chen, X., Lin, Z., Fang, D., and He, X. (2013) The structural basis of R-spondin recognition by LGR5 and RNF43. *Genes Dev. 27*, 1345−1350.

(28) Peng, W. C., de Lau, W., Forneris, F., Granneman, J. C., Huch, M., Clevers, H., and Gros, P. (2013) Structure of Stem Cell Growth Factor R-spondin 1 in Complex with the Ectodomain of Its Receptor LGR5. *Cell Rep. 3*, 1885−1892.

(29) Wang, D., Huang, B., Zhang, S., Yu, X., Wu, W., and Wang, X. (2013) Structural basis for R-spondin recognition by LGR4/5/6 receptors. *Genes Dev. 27*, 1339−1344.

(30) Xu, K., Xu, Y., Rajashankar, K. R., Robev, D., and Nikolov, D. B. (2013) Crystal structures of lgr4 and its complex with R-spondin1. *Structure 21*, 1683−1689.

(31) Hill, H. E., and Pioszak, A. A. (2013) Bacterial expression and purification of a heterodimeric adrenomedullin receptor extracellular domain complex using DsbC-assisted disulfide shuffling. *Protein Expression Purif. 88*, 107−113.

(32) Pioszak, A. A., and Xu, H. E. (2008) Molecular recognition of parathyroid hormone by its G protein-coupled receptor. *Proc. Natl. Acad. Sci. U.S.A. 105*, 5034−5039.

(33) Pioszak, A. A., Parker, N. R., Suino-Powell, K., and Xu, H. E. (2008) Molecular recognition of corticotropin-releasing factor by its G-protein-coupled receptor CRFR1. *J. Biol. Chem. 283*, 32900−32912.

(34) Kumar, S., Pioszak, A., Zhang, C., Swaminathan, K., and Xu, H. E. (2011) Crystal structure of the PAC1R extracellular domain unifies a consensus fold for hormone recognition by class B G-protein coupled receptors. *PLoS One 6*, e19682.

(35) Pal, K., Swaminathan, K., Xu, H. E., and Pioszak, A. A. (2010) Structural basis for hormone recognition by the Human CRFR2α G protein-coupled receptor. *J. Biol. Chem. 285*, 40351−40361.

(36) Pioszak, A. A., Parker, N. R., Gardella, T. J., and Xu, H. E. (2009) Structural basis for parathyroid hormone-related protein binding to the parathyroid hormone receptor and design of conformation-selective peptides. *J. Biol. Chem. 284*, 28382−28391.

(37) Kim, K. A., Wagle, M., Tran, K., Zhan, X., Dixon, M. A., Liu, S., Gros, D., Korver, W., Yonkovich, S., Tomasevic, N., Binnerts, M., and Abo, A. (2008) R-Spondin family members regulate the Wnt pathway by a common mechanism. *Mol. Biol. Cell 19*, 2588−2596.